DISCRETE ELEMENT ANALYSIS OF THE CORN THRESHING AND SEPARATION PROCESS

/

玉米籽粒脱粒分离过程离散元分析

Liquan YANG[1,2], Kun ZHAO[1], Guangyu YIN[3], Qianglong SU[1], Xiaodong LIU[1], Qingqing LÜ[1*], Zhe QU[2], Hongmei ZHANG[2] and Erbo LIU[1]

[1] Henan Province Engineering Research Center of Ultrasonic Technology Application, Pingdingshan University, Pingdingshan 467000, China;

[2] School of Mechanical and Electrical Engineering, Henan Agricultural University, Zhengzhou 450002, China;

[3] Pingdingshan Company, Henan Tobacco Company, Pingdingshan 467033, China;

** Corresponding author: Qingqing Lü*

Tel: +8618339975718; E-mail: 2696@pdsu.edu.cn

DOI: https://doi.org/10.35633/inmateh-78-07

Keywords: *Corn kernels, threshing process, discrete element method, orthogonal test*

ABSTRACT

This study focuses on the threshing device of a cross-axial flow drum and establishes a discrete element method (DEM) model to simulate the separation process of corn kernels within the device. The model reveals the motion behavior of corn kernels under different drum rotational speeds, feeding rates, and threshing gaps, as well as their spatial distribution along the axial direction of the drum. An orthogonal experimental design was employed to investigate the effects of various threshing parameters on the grain retention rate inside the device. The results indicate that drum rotational speed has the most significant influence on grain retention, followed by the feeding rate and the threshing gap. These findings provide an important theoretical basis for optimizing the threshing performance and improving the operational efficiency of the device. The optimal parameter combination was determined as follows: drum speed of 572.96 r/min, feeding rate of 1.5 kg/s, and threshing gap of 36 mm, which minimizes grain retention and ensures optimal operational performance.

摘要

以一种横轴流滚筒玉米脱粒机中的脱粒装置为研究对象，通过建立离散元模型来模拟玉米籽粒在脱粒装置中的分离过程，揭示了不同滚筒转速、籽粒喂入量、脱粒间隙下玉米籽粒的运动规律及玉米籽粒沿滚筒轴向的分布情况。通过正交试验揭示了不同脱粒条件对脱粒装置内部籽粒滞留率的影响，结果表明滚筒转速对籽粒滞留率的影响最大，其次是籽粒喂入量，最后是脱粒间隙。这对于优化脱粒装置的性能和提高其工作效率具有重要意义。最终确定的最优参数为：滚筒转速 572.96 r/min、籽粒喂入量 1.5 kg/s、脱粒间隙 36 mm，可以达到脱粒装置内最低的籽粒滞留率，从而实现最佳的作业效果。

1. INTRODUCTION

Corn cultivation occupies over 30% of China's total crop area. Since the 1980s, China's corn production has consistently grown, playing a vital role in the country's agricultural economy *(Zhang, 2022)*. Globally, corn is a major food and feed crop, second only to rice and wheat. Known for its high yield and stable output, corn is often referred to as the "king of feed" and is one of the most widely cultivated crops worldwide *(Mu, 2020; Liu et al., 2022; Vlădut et al., 2022)*. Given China's specific agricultural context, optimizing key parameters in the corn threshing process is essential for advancing corn production and processing technologies *(Zhang et al., 2023)*.

The discrete element method (DEM) has become a standard tool for analyzing particulate matter and its interactions with mechanical components, being widely applied in agricultural engineering *(Gao et al., 2024; Li et al., 2023; Wang et al., 2024)*.

Corn harvesters, particularly their threshing devices, are critical for mechanized corn production, significantly influencing harvesting efficiency *(Geng et al., 2023; Yuan, 2022; Yu et al., 2021)*. *Gong et al., (2024),* used EDEM discrete element simulation software to carry out simulation tests on different types of threshing drums and different threshing concave plates and corn ears with different round tube mounting angles, and finally determined the better threshing method.

Linrong Shi et al., (2022), investigated the effect of corn grain shape on the resting angle formation process by establishing a DEM model of corn kernels of three typical shapes. *Xiaoyu Li et al., (2024)*, validated the simulation results and test bench data through field experiments. They concluded that when the threshing drum speed was 356 r/min, the concave clearance was 40 mm, the installation spacing of the 50Mn steel rasp bars was 250 mm, and the feeding rate was 8 kg/s, the kernel breakage rate was 1.93%, which satisfies the requirements of the corn harvesting standard. It proves that DEM can be used to guide the optimization design of mechanical structures and has certain value for the research and development of other agricultural crop operation equipment. The study by *Kiniulis Valdas et al., (2017), Zhang et al., (2022),* showed that excessive grain feeding led to increased corn grain loss, and there was a positive correlation between feeding amount and threshing power consumption. Li Yaoming et al. improved the structure of the threshing device through the multi-factor orthogonal test method and optimized the key structural parameters, which effectively improved the harvest benefit of the threshing device *(Li et al., 2016)*. EDEM, as a practical discrete element simulation software, is in an indispensable position in the engineering field *(Liao et al., 2024; Yu et al., 2021; Li et al., 2025)*.

2. MATERIALS AND METHODS

2.1. Corn Threshing Drum Structure

In selecting a horizontal-axis flow thresher, the drum body is the core component that plays a vital role; its main function is to complete the threshing task. To facilitate the study of the movement and distribution of corn grains in the process of corn separation, the drum is divided into four sections: A, B, C and D. Among them, section A is 525 mm, section B is 433 mm, section C is 448 mm, section D is 254 mm, section A and B are mainly used for threshing, section C and D are used for screening and discharging *(Yang et al., 2022)*. The particle factory is set in section A, as shown in Figure 1(a), and the overall structural schematic of the device is presented in Figure 1.

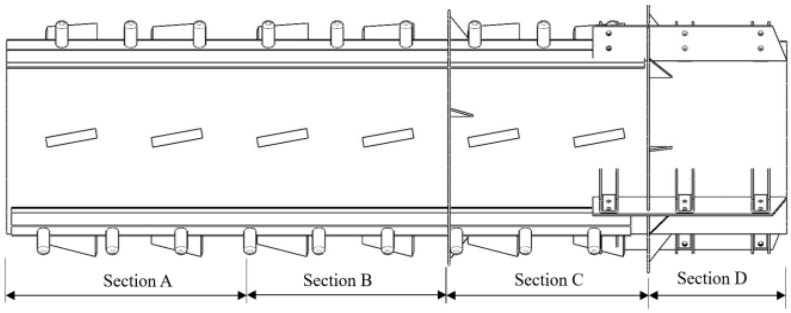

(a) Drum structure and functional segmentation

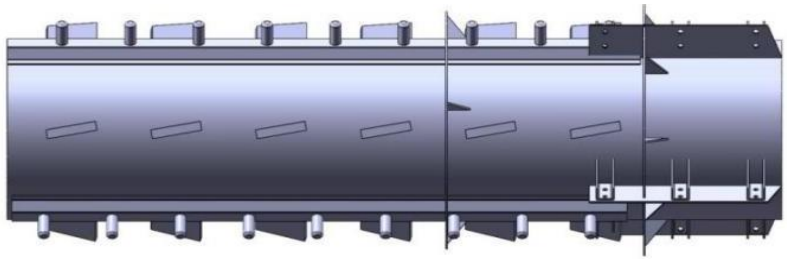

(b) Drum model

Fig. 1 - Structural schematic of the cross-axial flow threshing drum

2.2. Discrete Element Models

2.2.1 Threshing Device Model

The core components of a corn threshing device typically include a rotating threshing drum and a fixed concave. In practical operation, the concave remains stationary, while the threshing drum rotates at a prescribed speed to achieve the separation of corn kernels from the cob *(Yang, 2018)*. To improve the computational efficiency of the EDEM simulations (Altair EDEM 2023), the device geometry was appropriately simplified by removing non-critical structures, while retaining the essential components, namely the threshing drum and the concave. This simplification ensures that the simulation process can accurately represent the actual threshing behavior of the machine.

In addition, the cylinder shaft, cylinder, cylinder teeth, plate teeth, partition plates, miscellaneous plates, and other components inside the drum were merged into a single entity, and a three-dimensional model of the simplified threshing device was generated. The model was saved in *.STL format and imported into EDEM, as shown in Figure 2.

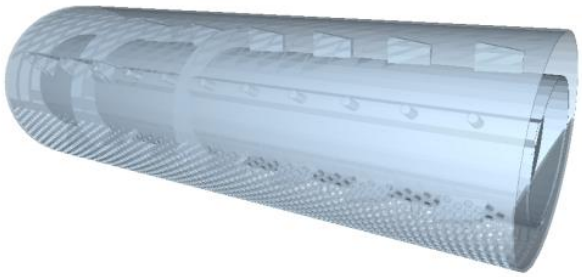

Fig. 2 - Discrete meta-model of the corn threshing device

2.2.2. Discrete Meta-model of Corn Kernels

In this study, Zhengdan 958 corn varieties were selected, 80 corn kernels were selected as samples, and the length, thickness, and width of each kernel were repeatedly measured *(Tang et al., 2024)* by a vernier caliper. The measured data were used to calculate the average value of each dimension, as presented in Table 1.

Table 1

Geometric dimensions of Zhengdan 958 corn kernels

Length [mm]	**Top Width** [mm]	**Root width** [mm]	**Thickness** [mm]
10.28	8.14	6.23	4.33

To improve the computational efficiency of the simulation, an appropriate particle size was preset before importing the model into the EDEM software. Accordingly, spherical particles with a minimum radius of 0.50 mm were selected for particle filling, forming a discrete kernel model. Each kernel was represented by 106 spherical particles *(Chen et al., 2024)*. The particle filling process of the corn kernels is shown in Figure 3.

(a) Three-dimensional model; (b) Discrete element models; (c) Particle filling model

Fig. 3 - Corn grain particle filling process

2.2.3. Discrete Element Model Parameters

In the discrete element model, the mechanical and physical properties of corn kernels and the threshing device were defined according to *Wang et al. (2018)*, as listed in Table 2.

Table 2

Parameter settings for the EDEM simulation

Parameter	**Value**
Poisson's ratio of corn kernels	0.4
Shear modulus of corn kernels [Pa]	1.31×10^{8}
Density of corn kernels [kg·m^{-3}]	1430
Coefficient of restitution (kernel–kernel)	0.151
Static friction coefficient (kernel–kernel)	0.086
Rolling friction coefficient (kernel–kernel)	0.072
Poisson's ratio of alloy tool steel	0.25
Shear modulus of alloy tool steel [Pa]	8×10^{10}
Density of alloy tool steel [kg·m^{-3}]	7850

Parameter	Value
Coefficient of restitution (kernel–steel)	0.702
Static friction coefficient (kernel–steel)	0.344
Rolling friction coefficient (kernel–steel)	0.053

2.3. *Study on selected material properties of corn kernels*

2.3.1. Effect of Kernel Moisture Content on the Angle of Repose

The angle of repose is an important physical parameter used to characterize the flowability and frictional behavior of granular materials, such as corn kernels. It directly reflects the piling behavior of particulate materials and is a simple and convenient index for experimental measurement *(Ma et al., 2024; Mousaviraad et al., 2022)*. In discrete element method (DEM) simulations, the angle of repose is commonly employed to validate the accuracy of contact models and parameter calibration *(Chen et al., 2023)*. This parameter is essential for understanding the behavior of corn kernels during storage, handling, and processing, and it provides a theoretical basis for the optimization of these processes *(Mu, 2022; Li et al., 2022; Vlădut et al., 2023)*.

When the Johnson-Kendall-Roberts (JKR) contact model is adopted to describe interparticle interactions, the effects of electrostatic forces and van der Waals forces can be neglected, and the liquid bridge force becomes the dominant interaction force *(Mu et al., 2020)*. When the particle surfaces are wet or contain moisture, the formation of liquid bridges can significantly affect the aggregation behavior and flow characteristics of the particles *(Zou et al., 2016; Wu, 2019)*. By neglecting the influence of the self-weight of the liquid bridge on the static liquid bridge force, and according to the formulations reported in the relevant literature for wet-particle DEM, the static liquid bridge force can be expressed by Eqs. (1)–(3) *(Chen et al., 2020)*. A schematic of the liquid bridge formed between two wet spherical particles is shown in Figure 4.

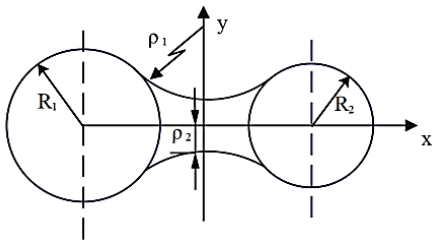

Fig. 4 - Wet particle contact model

The capillary pressure of the liquid bridge is expressed as:

$$P = \left[\frac{y''}{(1+y')^{\frac{3}{2}}} - \frac{1}{y(1+y')^{\frac{1}{2}}} \right] \sigma \tag{1}$$

where: P is the capillary pressure of the liquid bridge, N; y is the coordinate along the *y*-axis, mm; σ is the surface tension of the liquid, N/m.

Since the analytical solution of Eq. (1) is not straightforward, the ring approximation method is adopted to calculate the static liquid bridge force.

The corresponding expression is given as follows:

$$\begin{cases} F_s = 2\pi\rho_2\sigma \\ F_p = P\pi\rho_2^2 \end{cases} \tag{2}$$

The static liquid bridge force can be expressed as:

$$F = \pi\sigma\rho_2 \frac{\rho_1 + \rho_2}{\rho_1} \tag{3}$$

where:

F_S is the surface tension of the liquid, N; F_P is the static pressure, N;

ρ_1, ρ_2 is the maximum and minimum radius of curvature of the liquid bridge.

2.3.2. Experimental Design and Pretreatment

In the numerical simulation of the angle of repose of corn kernels using EDEM software, the JKR contact model, which is suitable for wet materials, was adopted. This choice was made because the simulation involves contact interactions between moist particles, and agglomeration phenomena may occur between them. In both the numerical simulation and the physical experiment, the same bottomless cylinder method was employed to measure the angle of repose. The operating procedures were identical for the simulation and the experimental tests. In this method, the diameter of the bottomless cylinder was 60 mm, and its height was 180 mm, corresponding to a diameter-to-height ratio of 1:3. To prevent kernel overflow during particle generation in the particle factory, which could affect the accuracy of the results, the height of the bottomless cylinder in the simulation was increased to 200 mm.

2.3.2.1. Simulation Test Procedure

Using the Protractor measurement tool in EDEM, three representative corn kernels were manually selected at appropriate positions on the front view of the particle pile to determine the angle of repose.

The measurements were repeated three times, and the arithmetic mean value was calculated. The measurement procedure is illustrated in Figure 5.

(a) Kernel filling (b) Filling completed (c) Lifting of the cylinder (d) Pile formation completed

Fig. 5 - Simulation process of corn kernel pile formation for angle of repose measurement

2.3.2.2. Physical Test Procedure

The corn kernels used in the physical experiments were prepared based on the kernel shape generated in the simulation. The experimental method and procedure were generally consistent with those used in the numerical simulation, as shown in Figure 6.

Fig. 6 - Physical test procedure for the formation of a corn kernel pile

The calculation formula for the angle of repose of corn kernels is given as follows:

$$\beta = \arctan \frac{2h}{l} \tag{4}$$

where: β is the angle of repose of corn kernels; h is the height of the kernel pile, mm; l is the base diameter of the kernel pile, mm.

2.3.3. Angle of Repose Analysis

Figure 7 shows the simulated pile formation of corn kernels under different moisture contents, while Figure 8 presents the corresponding experimental results. The angle of repose was determined using the measurement tools in the EDEM software and the calculation method employed in the physical experiments.

(a) Angle of repose test (dry kernels) (b) Angle of repose test (wet kernels)

Fig. 7 - Simulation results

(a) Angle of repose test (dry kernels) (b) Angle of repose test (wet kernels)

Fig. 8 – Experimental results

According to the simulation results, the angle of repose of dry corn kernels was 19.4°, whereas that of wet corn kernels was 35.6°. In the physical experiments, the corresponding values were 18.9° for dry kernels and 36.3° for wet kernels. The detailed results are summarized in Table 3.

Table 3

Comparative results of the angle of repose for corn kernels

Experiment number	Dry corn kernels		Moist corn kernels	
	Simulation angle [°]	Experimental angle [°]	Simulation angle [°]	Experimental angle [°]
1	19.6	19.0	36.2	36.6
2	18.7	18.2	35.5	36.9
3	19.9	19.5	35.1	35.4
Average [°]	19.4	18.9	35.6	36.3
Standard deviation [°]	0.62	0.66	0.55	0.79

The moisture content of the particles was measured using a grain moisture meter (model PM8188). The moisture content of the dry corn kernels was 13.6%, while that of the moist kernels was 38.2%. When the kernels are in a dry state, the absence of liquid bridge forces results in relatively low interparticle friction, leading to poor pile stability. In contrast, when the kernels contain a certain amount of moisture, liquid bridge forces are formed between particles, which promote particle agglomeration and significantly enhance the stability of the kernel pile.

2.4. Discrete element simulation of the threshing process

2.4.1. Establishment of the simulation model

The *.STL file of the corn kernel model was imported into the EDEM software. In EDEM, the coordinate system was defined with respect to the cross-axial flow drum. Specifically, the drum axis direction was set along the negative *Z*-axis, the horizontal radial direction of the drum was aligned with the *X*-axis, and the vertically downward radial direction was defined as the negative *Y*-axis. According to the data presented in Table 2, the physical and mechanical parameters of the corn kernels and the threshing device were assigned, including Poisson's ratio, density, elastic modulus, friction coefficients, and coefficients of restitution for particle-particle and particle-machine contacts *(Dong et al., 2023)*. The direction of gravitational acceleration was specified according to the simulation requirements. Considering that corn kernels behave as non-adhesive particles and that their interactions are primarily governed by small elastic deformations at the contact interfaces, the Hertz-Mindlin (no-slip) contact model was adopted to describe both kernel-kernel and kernel-machine interactions *(Li et al., 2022)*. Subsequently, mesh partitioning was performed, and the particle factory was configured to generate kernels with the prescribed properties *(Zhao, 2019; Li, 2021; Tian et al., 2022)*.

To replicate the process from fresh harvesting to entry into the threshing apparatus, an initial downward velocity of 0.3 m/s was assigned to the corn kernels.

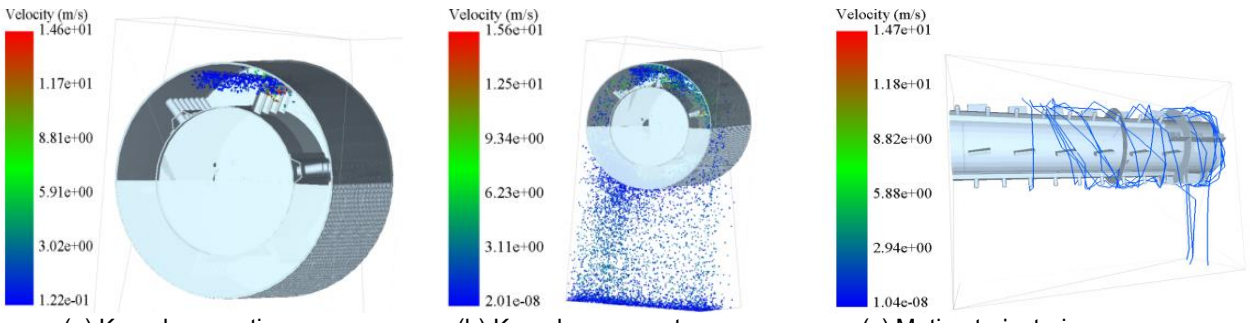

(a) Kernel generation (b) Kernel movement (c) Motion trajectories

Fig. 9 - Discrete element simulation of the corn kernel threshing process

Figure 9(a) illustrates the kernel generation process. At this stage, when a large number of particles are generated by the particle factory, they immediately interact with the rotating drum. As shown in Figure 9(b), the kernels are generated, impacted by the drum, pass through the threshing concave, and subsequently exit the threshing system.

To investigate the motion behavior of corn kernels within the drum, several kernels exhibiting long axial displacement were selected in EDEM, and their motion paths were converted into trajectories. For ease of visualization, different colors were assigned to the trajectories *(Wang et al., 2019)*, as shown in Figure 9(c).

It can be observed that after being generated by the particle factory, the kernels undergo circumferential rotation while moving along the axial direction of the drum, and eventually exit the threshing concave at the end of the device under the action of gravity. The simulation results are in good agreement with the actual operating conditions.

2.4.2. Determination of Simulation Factors

In this study, three key parameters were considered: the rotational speed of the drum, the kernel feeding rate, and the axial distribution of kernels within the drum *(Li et al., 2023; Geng et al., 2019)*. By systematically varying these parameters and analyzing their effects on kernel motion and distribution, the threshing process can be optimized to enhance both efficiency and performance *(Wang et al., 2020)*. To ensure that the simulation conditions were consistent with practical operating conditions, the drum rotational speed was set to four levels: 40 rad/s, 50 rad/s, 60 rad/s, and 70 rad/s, corresponding to 381.97 r/min, 477.46 r/min, 572.96 r/min, and 668.45 r/min, respectively. The kernel feeding rate was specified in kg/s, with an initial value of 1.5 kg/s and a step size of 0.3 kg/s, resulting in four levels: 1.5 kg/s, 1.8 kg/s, 2.1 kg/s, and 2.4 kg/s. The threshing gap was selected within the range of 33–42 mm, with a step size of 3 mm. Accordingly, four levels were defined: 33 mm, 36 mm, 39 mm, and 42 mm *(Wang et al., 2022)*. The specific parameter levels are summarized in Table 4.

Table 4

Levels of simulation factors for the Zhengdan 958 corn kernels

Levels	Factors		
	Drum rotational speed [r/min]	**Kernel feeding rate** [kg/s]	**Threshing gap** [mm]
1	381.97	1.5	33
2	477.46	1.8	36
3	572.96	2.1	39
4	668.45	2.4	42

Based on the grid division of the designated sampling box, the number of corn kernels within each grid can be counted, as shown in Figure 10.

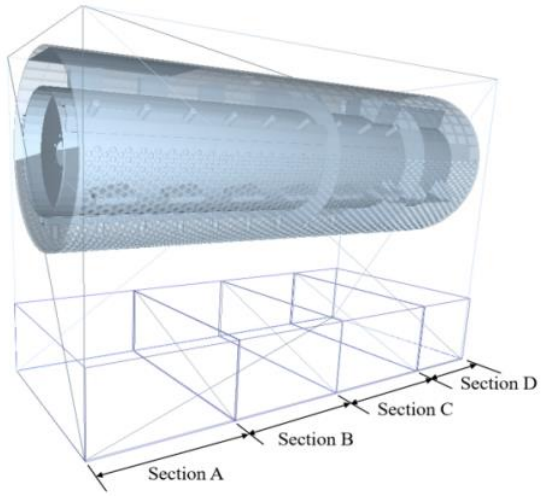

Fig. 10 - Grid division of the threshing device

The axial distribution curves of corn kernels under different influencing factors were analyzed based on the following test results *(Yu, 2013)*.

3. RESULTS

3.1 Simulation results analysis

3.1.1 Simulation Results for Different Drum Speeds

The kernel feeding rate was set to 2.1 kg/s, and the threshing gap was fixed at 36 mm. The corresponding axial distribution curves under different drum speeds are shown in Figure 11.

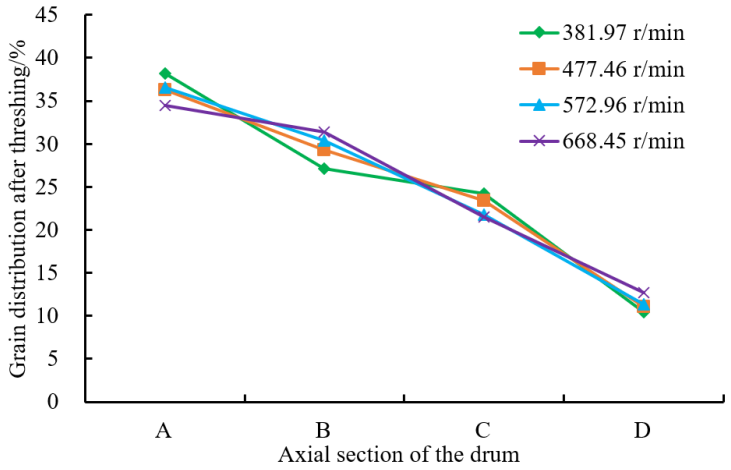

Fig. 11 - Axial distribution of corn kernels at different drum speeds

Based on the analysis of the axial distribution curves, the following conclusions can be drawn:

1. Since the particle factory was located in Section A during the simulation, corn kernels were generated in this section, resulting in the highest kernel concentration in this region.

2. When the drum speed was 381.97 r/min, the proportion of corn kernels in Section A reached a maximum of 38.18%, mainly due to the dominant influence of gravity. In contrast, when the drum speed increased to 668.45 r/min, the proportion of kernels in Section A decreased to a minimum of 34.42%, indicating that higher rotational speeds promote longer axial transport distances.

3. At all four drum speeds, the kernel distribution gradually decreased along the axial direction. Among them, at a drum speed of 572.96 r/min, the axial distribution curve exhibited the most uniform trend, whereas the distributions under the other three conditions showed more pronounced fluctuations.

Further analysis indicates that with increasing rotational speed, the combined effects of centrifugal force and axial thrust become more significant. The enhanced centrifugal force facilitates the backward transport of kernels along the drum axis. Moreover, at higher rotational speeds, the frequency and energy of impacts between the threshing teeth and the kernels increase, thereby accelerating the axial movement of the kernels.

3.1.2 Simulation Results for Different Kernel Feeding Rates

The drum rotational speed was fixed at 572.96 r/min, and the threshing gap was set to 36 mm. The corresponding axial distribution curves of corn kernels under different feeding rates are shown in Figure 12.

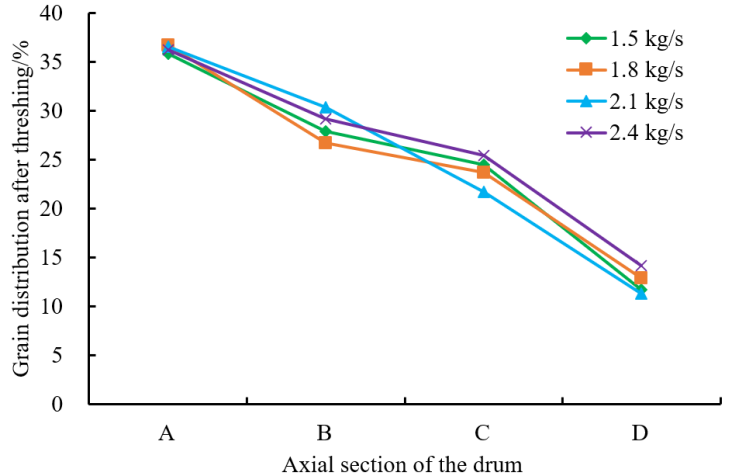

Fig. 12 - Axial distribution of corn kernels under different feeding rates

Due to the presence of the annular baffle, the number of kernels in Section C is lower than that in Section B. When the kernel feeding rates were 1.5 kg/s, 1.8 kg/s, and 2.4 kg/s, the axial distribution curves in Sections B and C exhibited relatively gentle variations. Under all four feeding conditions, the kernel distribution gradually decreased along the axial direction, and the rate of decrease was generally similar. This indicates that the feeding rate had a limited influence on the overall axial distribution of kernels.

It can be inferred that within the feeding rate range considered in this study (1.5–2.4 kg/s), the threshing and conveying capacities of the drum were sufficient to handle different material loads without causing distribution irregularities due to overload. Although a slight increase in resistance may occur at higher feeding rates due to enhanced inter-kernel compression, this effect does not significantly alter the overall motion trajectories of the kernels.

3.1.3. Simulation Results for Different Threshing Gaps

The drum rotational speed was fixed at 572.96 r/min, and the kernel feeding rate was set to 2.1 kg/s. The corresponding axial distribution curves of corn kernels under different threshing gaps are shown in Figure 13.

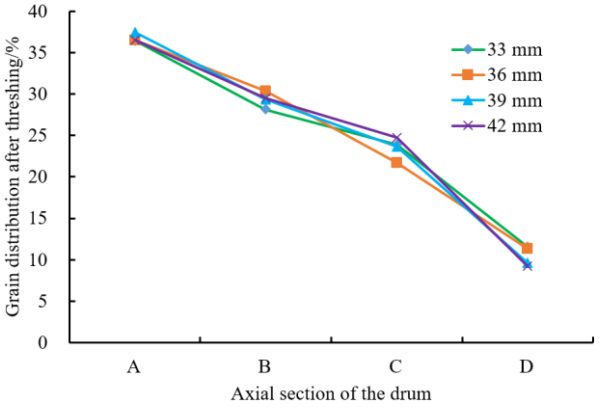

Fig. 13 - Axial distribution of corn kernels under different threshing gaps

At threshing gaps of 39 mm and 42 mm, the proportion of corn kernels in Section D decreased most significantly, reaching approximately 9%. This indicates that as the threshing gap increases, the contact between the kernels and the concave decreases, resulting in a shorter axial transport distance and earlier exit of the kernels from the threshing system.

With an increasing threshing gap, the residence time of the kernels on the concave surface is reduced, thereby decreasing the axial displacement induced by frictional forces and repeated impacts. Although an excessively large gap may potentially lead to incomplete threshing, no significant losses were observed in the present simulations due to the appropriate matching of feeding rate and rotational speed. In addition, increasing the threshing gap alters the material flow density distribution between the drum and the concave, which may make the kernels more susceptible to entrainment by airflow or subsequent premature discharge.

5.1.4. Multifactor Orthogonal Experimental Design

An orthogonal experimental design is an efficient method for investigating the effects of multiple factors at multiple levels, identifying the dominant factors, and determining the optimal parameter combinations for system optimization. This method is characterized by factor independence, uniform distribution of test points, convenient experimental design, a reduced number of trials, and stable and reliable results *(Liu et al., 2023; Qiao et al., 2022)*.

In the harvesting of breeding corn, it is necessary not only to meet the operational requirements of threshing, but also to minimize kernel stagnation and mixing within the device. In this context, the kernel retention rate inside the threshing device should be no greater than 5%. Therefore, this study aims to optimize the kernel retention rate by adjusting the drum rotational speed, kernel feeding rate, and threshing gap, thereby improving the overall threshing performance. The kernel retention rate in the threshing device was adopted as the evaluation index *(Li et al., 2016)*, and it is calculated as follows:

$$C = \frac{m}{M} \times 100\% \tag{5}$$

where: C is the kernel retention rate; m is the mass of retained kernels, kg; M is the total mass of the fed material, kg.

The orthogonal experimental matrix was designed based on the selected factor levels. Since a standard orthogonal table for three factors at four levels is not directly available, the L_{16} (4^5) orthogonal array was adopted and appropriately simplified to accommodate the three-factor, four-level experimental design. As a result, a total of 16 simulation runs were required. The simulation tests were conducted by varying three factors: drum rotational speed (r/min), kernel feeding rate (kg/s), and threshing gap (mm). Each factor was assigned four levels, and the simulation duration for each run was set to 6 s. The orthogonal array and the corresponding simulation scheme, along with the obtained results, are presented in Table 5.

Table 5

Orthogonal simulation scheme and results

Test Number	Drum speed [r/min]	Kernel Feeding Rate [kg/s]	Threshing gap [mm]	Kernel retention rate [%]
1	381.97	1.5	33	0.29
2	381.97	1.8	36	0.34
3	381.97	2.1	39	0.32
4	381.97	2.4	42	0.25
5	477.46	1.5	36	0.20
6	477.46	1.8	33	0.39
7	477.46	2.1	42	0.41
8	477.46	2.4	39	0.40
9	572.96	1.5	39	0.19
10	572.96	1.8	42	0.28
11	572.96	2.1	33	0.24
12	572.96	2.4	36	0.19
13	668.45	1.5	42	0.32
14	668.45	1.8	39	0.17
15	668.45	2.1	36	0.30
16	668.45	2.4	33	0.31

To ensure high harvesting quality and operational efficiency, the amount of corn kernels retained within the threshing device should be minimized, and the kernel retention rate should be reduced as much as possible. The degree of influence of each factor on the kernel retention rate can be evaluated using range analysis. The corresponding results of the range analysis are presented in Table 6.

Table 6

Range analysis of kernel retention rate

Level	Kernel retention rate [%]		
	Drum rotational speed [r/min]	**Kernel feeding rate** [kg/s]	**Threshing gap** [mm]
k1	0.300	0.250	0.307
k2	0.350	0.295	0.258
k3	0.225	0.318	0.270
k4	0.275	0.288	0.315
Range	0.125	0.068	0.057

A comprehensive analysis indicates that the optimal parameter combination is a drum rotational speed of 572.96 r/min, a kernel feeding rate of 1.5 kg/s, and a threshing gap of 36 mm. This optimal combination provides the best overall operational performance and minimizes the kernel retention rate within the threshing device.

4. CONCLUSIONS

Taking the cross-axial flow drum threshing device as the research object, this study established a corn kernel threshing and separation simulation model based on the Discrete Element Method. The effects of key operating parameters, including drum rotational speed, kernel feeding rate, and threshing gap, on the axial distribution of kernels were systematically investigated. In addition, the intrinsic relationship between kernel moisture content and accumulation behavior was analyzed. Furthermore, an orthogonal experimental design was employed to optimize the operating parameters of the threshing device with the objective of minimizing the kernel retention rate.

Based on the comprehensive results obtained from numerical simulations and experimental validation, the following conclusions can be drawn:

1. The axial distribution of corn kernels along the drum was analyzed under different operating conditions. The results indicate that increasing the drum rotational speed leads to a higher proportion of kernels reaching the rear section of the drum. In contrast, enlarging the threshing gap weakens the axial transport effect. The reduced contact area between the kernels and the threshing components shortens the interaction time, causing the kernels to exit the threshing system earlier.

2. The influence of kernel moisture content on the angle of repose was systematically investigated. The results demonstrate that moisture differences significantly affect the accumulation behavior of granular materials. The formation of liquid bridge forces between wet kernels enhances interparticle adhesion and friction, thereby improving pile stability and resulting in a larger angle of repose.

3. Based on the orthogonal experimental analysis, the effects of drum speed, kernel feeding rate, and threshing gap on the kernel retention rate were evaluated. The optimal parameter combination was identified as a drum speed of 572.96 r/min, a kernel feeding rate of 1.5 kg/s, and a threshing gap of 36 mm. This combination ensures optimal operational performance of the threshing device and minimizes kernel retention, thereby improving overall threshing efficiency.

ACKNOWLEDGEMENT

This research was funded by the Key R&D and Promotion Special/Tackling Key Problems in Science and Technology in Henan Province, China (grant No. 242102111173, 242102111172, 242102110365, 242102110378, 252102110351); Key Scientific Research Fund of Pingdingshan University (grant No. PXY-JXZDXK-202306, 2023-JYZD01).

REFERENCES

[1] Zhang N., (2022). *Research on working mechanism and optimization analysis of chaffer sieve cleaning device in corn grain harvester (玉米籽粒收获机鱼鳞筛清选装置工作机理及优化分析)*. Master's Thesis, Jilin University, Changchun, China.

[2] Mu P.L., (2020). *Research on high net and low loss cleaning screen of corn grain harvester. Master's Thesis (玉米籽粒收获机械高净低损清选筛研究)*. Jilin University, Changchun, China.

[3] Liu X.Z., Li M., Zhang J., Chen R.J., Fu H., Ma G.M., Zhou Y.H., Zhuang X.L., (2022). The dehydration and mechanical-harvesting of maize grain: Research progress (玉米籽粒脱水及机收籽粒研究进展). *Journal of Agriculture*, 12(7), 64-68.

[4] Vlădut N.V., Biris S.St., Cârdei P., Găgeanu I., Cujbescu D., Ungureanu N., Popa L.D., Perişoară L., Matei G., Teliban G.C., (2022). Contributions to the Mathematical Modeling of the Threshing and Separation Process in An Axial Flow Combine, *Agriculture*, 12(10), 1520.

[5] Zhang W., Jin F., Li Q.X., Zhang J.S., Zhai X.P., Wang S.B., (2023). Design and experiment of cleaning device for corn grain combine harvester (玉米籽粒联合收获机清选装置优化设计与试验). *Xinjiang Agricultural Sciences*, 60(12), 3102-3112.

[6] Gao P.F., Zhang X.W., Jiang C.X., Yi K.C., Zhang X.L., Ma Z.W., (2024). Optimized design and test of axial roller fresh corn threshing device (轴向滚筒式鲜食玉米脱粒装置优化设计与试验). *Journal of Agricultural Machinery*, 55(S2), 145-156.

[7] Li X.Y., Du Y.F., Mao E.R., Zhang Y.A., Liu L., Guo D.F., (2023). Design and experiment of corn low damage threshing device based on DEM (玉米低损籽粒直收机自动控制系统设计与试验). *International Journal of Agricultural and Biological Engineering*, 16(3), 55-63.

[8] Wang J., Li L.J., Shi W.L., Ding Y.Q., (2024), Study on the operating effect of straw crushing and spreading devices on single axial flow harvesters, *INMATEH-Agricultural Engineering*, 75(1), 480-489.
[9] Geng D., Sun Y., Wang Z., Wang Q.H., Ming J.R., Yang H.L., Xu H.G., (2023). Design and experiment of plate tooth threshing device of corn grain direct harvester (玉米籽粒直收机板齿式脱粒装置设计与试验). *Journal of Jilin University (Engineering and Technology Edition)*, 53(11), 3281-3292.
[10] Yuan H.K., (2022). *Research on the mechanism and bionic key technology of corn mechanical threshing to reduce losses and increase efficiency (玉米脱粒降损增效机理与仿生关键技术研究)*. Doctoral Thesis, Jilin University, Changchun, China.
[11] Yu Y.J., Li L.S., Zhao J.L., Wang X.G., (2021). Discrete element simulation based on elastic–plastic damping model of corn kernel–cob bonding force for rotational speed optimization of threshing component. *Processes*, 9(8): 1410.
[12] Gong J.L., Luo Z.J., Zhang Y.F., (2024). Optimised design and simulation analysis of longitudinal flow corn cone threshing device. *INMATEH-Agricultural Engineering*, 73(2), 63-70.
[13] Shi L.R., Zhao W.Y., Yang X.P., (2022). Effects of typical corn kernel shapes on the forming of repose angle by DEM simulation. *International Journal of Agricultural and Biological Engineering*, 15(2), 248-255.
[14] He Y.Z., Wang M.X., Wang W., Li S.B., (2024). Simulation research on the transfer and collection part of warehouse bottom surplus grain cleaning device(平房仓仓底余粮清扫装置传送及收集仿真研究). *Food and Machinery*, 40(2), 91-96.
[15] Kiniulis V., Steponavičius D., Andriušis A., Kemzūraitė A., Jovarauskas D., (2017). Corn ear threshing performance of filler-plate-covered threshing cylinders. *Mechanics*, 23(5), 714-722.
[16] Zhang N., Fu J., Wang R.X., Chen Z., Fu Q.K., Chen X.G., (2022). Experimental study on the particle size and weight distribution of the threshed mixture in corn combine harvester. *Agriculture*, 12(8), 1214.
[17] Li Y.M., Chen Y., Xu L.Z., Li L., (2016). Optimization of structural parameters for threshing and separating device in oblique tangential-longitudinal combine (斜置切纵流联合收获机脱粒分离装置结构参数优化). *Transactions of the Chinese Society of Agricultural Machinery*, 47(9), 56-61.
[18] Zhao Y.Q., Chen Z.X., Zhao W., Li S.M., Jiao Y.J., Hu C., Zhang Y., (2025). Calibration of simulation parameters for silage corn straw material based on discrete element method (基于离散元法的青贮玉米粉碎物料仿真参数标定). *Feed industry*, 46(19), 9-16.
[19] Liao Y.L., Zhao Y.H., Yuan S., Li F.F., Ye C.C., Chen H.B., Chen R.F., (2024). Discrete element model establishment and parameter calibration of maize seeds (玉米种子离散元模型建立及参数标定). *Jiangsu Agricultural Science*, 52(18), 209-214.
[20] Yu Y.J., Li L.S., Zhao J.L., Wang X.G., Fu J., (2021). Optimal design and simulation analysis of spike tooth threshing component based on DEM. *Processes*, 9(7), 1163.
[21] Li M.R., Yao Y.C., Zhu Y.K., Li X.B., Yue, D., Geng D.Y., (2025). Design and experiment of a double longitudinal axial-flow corn threshing device for large feeding capacity, *INMATEH-Agricultural Engineering*, 75(1), 527-538.
[22] Yang L.Q., Lü Q.Q., Zhang H.M., (2022). Experimental study on direct harvesting of corn kernels. *Agriculture*, 2022, 12(7), 919.
[23] Yang L.Q., (2018). *Design and experiment research based on tangential flow transverse axial flow corn threshing system (切流横轴流玉米脱粒系统设计及试验研究)*. Doctoral Thesis, Henan Agricultural University, Zhengzhou, China.
[24] Tang Q., Jiang L., Yu W.Y., Wu J., Wang G. (2024). Design and experiment of high moisture corn threshing device with low damage. *INMATEH-Agricultural Engineering*, 74(3), 172-183.
[25] Chen Z.R., Liu Z.B., Guan W., Guo J.B., Xue D.M. (2024). Maize grain modelling for the DEM simulation of sowing process (面向播种过程离散元仿真的玉米颗粒建模方法). *Transactions of the Chinese Society of Agricultural Engineering*, 40(14), 14-22.
[26] Wang M.M., Wang W.Z., Yang L.Q., Hou M.T. (2018). Research of discrete element modeling method of maize kernel based on EDEM (基于 EDEM 的玉米子粒建模方法的研究). *Journal of Henan Agricultural University*, 52(1), 80-84.
[27] Ma S.K., He X.N., Zhu H., Liu Z.X., Wang D.W., Shang S.Q., Li G.H. (2024). Vibration parameter calibration and test of tiger nut based on discrete element method. *INMATEH-Agricultural Engineering*, 73(2), 30-39.

[28] Mousaviraad M., Tekeste M.Z. (2022). Effect of grain moisture content on physical, mechanical, and bulk dynamic behavior of maize. *Biosystems Engineering*, 195, 186-197.
[29] Chen Z.P., Wassgren C., Ambrose, R.K. (2023). Development and validation of a DEM model for predicting compression damage of maize kernels. *Biosystems Engineering*, 230, 480-496.
[30] Mu X.D. (2022). *Study and experiment on crushing mechanism of whole silage maize based on dish roller (基于碟盘辊的全株青贮玉米破碎机理研究与试验)*. Master's Thesis, Shandong University of Technology, Zibo, China.
[31] Li H.C., Zeng R., Yang T.Y., Niu Z.Y. (2022). Experimental study on the impact breakage characteristics of maize kernels (玉米籽粒冲击破碎特性试验研究). *Transactions of the Chinese Society of Agricultural Engineering*, 38(7), 29-37.
[32] Vlădut N.V., Ungureanu N., Biris S. St., Voicea I., Nenciu F., Găgeanu I., Cujbescu D., Popa L.D., Boruz S., Matei G., Ekielski A., Teliban G.C. (2023). Research on the identification of some optimal threshing and separation regimes in the axial flow apparatus, *Agriculture*, 13(4), 838.
[33] Mu X.D., Jiang H.X., Sun Y.C., Xu H.G., Yao Y.C., Geng D.Y. (2020). Simulation optimization and experiment of disc-type grain crushing device of silage corn harvester (青贮玉米收获机碟盘式籽粒破碎装置仿真优化与试验). *Transactions of the Chinese Society for Agricultural Machinery*, 51(s1), 218-226.
[34] Zou Q.R., Zhang W. (2016). Experimental study on the physical characteristics of corn germination (玉米芽种物理特性试验研究). *Journal of Heilongjiang Bayi Agricultural Reclamation University*, 28(04), 79-84.
[35] Wu B.X. (2019). *Study on the physical and mechanical properties of frozen maize grains(冻玉米籽粒物理力学特性研究)*. Master's Thesis, Northeast Agricultural University, Harbin, China.
[36] Che, G.Q., Yan J.X., Zhang L.R. (2020). Discrete element method simulation of corn grain stacking characteristics (玉米颗粒堆积特性的离散元法模拟研究). *Light Industry Machinery*, 38(06), 11-14.
[37] Dong J.Q., Zhang D.X., Yang L., Gui T., Zhang K.L. (2023). Discrete element method optimisation of threshing components to reduce maize kernel damage at high moisture content. *Biosystems Engineering*, 233, 221-240.
[38] Li X.Y., Du Y.F., Liu L., Mao E.R., Yang F. (2022). Research on the constitutive model of low-damage corn threshing based on DEM. *Computers and Electronics in Agriculture*, 194, 106722.
[39] Zhao L. (2019). *Development and experiment of low-feeding high moisture corn threshing device (低喂入量高湿玉米脱粒装置的研制与试验)*. Master's Thesis, Sichuan Agricultural University, Yaan, China.
[40] Li K. (2021). *Design and experimental research on the vertical axial flow corn seed direct harvest threshing device (纵轴流玉米籽粒直收脱粒装置的设计与试验研究)*. Master's Thesis, Northeast Agricultural University, Taian, China.
[41] Tian Z.W., Ma W., Yang Q.C., Yao S., Guo X.Y., Duan F.M. (2022). Design and experiment of gripper for greenhouse plug seedling transplanting based on EDM. *Agronomy*, 12(7), 1487.
[42] Wang M.M., Wang W.Z., Yang L.Q., Zhang H.M., Zhong D.F. (2019). Bench experiment and discrete element simulation analysis of corn threshing process (玉米脱粒过程台架试验与离散元仿真分析). *Journal of Henan Agricultural University*, 53(03), 365-373.
[43] Li H.B., Wang Q.H., Ma J., Wang Y.N., Yue D., Geng D.Y. (2023). Design and experiment of transverse axial flow corn flexible threshing device. *INMATEH-Agricultural Engineering*, 2023, 69(01), 461-470.
[44] Geng D.Y., He K., Wang Q., Jin C.Q., Zhang G.H., Lu X.F. (2019). Design and experiment on transverse axial flow flexible threshing device for corn (横轴流式玉米柔性脱粒装置设计与试验). *Transactions of the Chinese Society of Agricultural Machinery*, 50(3), 101-108.
[45] Wang Q.R., Mao H.Q., Li Q.L. (2020). Modelling and simulation of the grain threshing process based on the discrete element method. *Computers and Electronics in Agriculture*, 178: 105790.
[46] Wang L.J., Liu W.T., Li Y.H., Yu K.M. (2022). Research on double-layer jitter plates with holes in large-feeding mass cleaning system of maize grain harvester (大喂入量玉米籽粒收获机清选系统双层筛孔抖动板研究). *Transactions of the Chinese Society of Agricultural Machinery*, 53(7), 92-102.
[47] Yu Y.J. (2013). *Research on analysis method of corn threshing based on 3D DEM (基于三维离散元法的玉米脱粒过程分析方法研究)*. Doctoral Thesis, Jilin University, Changchun, China, 2013.

[48] Liu Y.C., Li, M.H., Wang J.Z., Feng L., Wang F.Z., He X.N. (2023). Design and test of entrainment loss detection system for corn kernel direct harvester (玉米籽粒直收机夹带损失检测系统设计与试验). *Transactions of the Chinese Society of Agricultural Machinery*, 54(05), 140-149.

[49] Qiao M.M., Xia G.Y., Cui T., Xu Y., Fan C.L., Su Y., Li Y.B., Han, S.Y. (2022). Machine learning and experimental testing for prediction of breakage rate of maize kernels based on components contents. *Journal of Cereal Science*, 108, 103582.

[50] Li X.K., Han Z.S., Dai F., Gao A.M., Wei L.J. (2016). Simulation research on working parameters of threshing device on plot-bred wheat based on EDEM (基于 EDEM 的小区育种小麦脱粒装置作业参数仿真研究). *Agricultural Research in the Arid Areas*, 34(04), 292-298.